Intracellular Retention of the NKG2D Ligand MHC Class I Chain-Related Gene A in Human Melanomas Confers Immune Privilege and Prevents NK Cell-Mediated Cytotoxicity[1]

Mercedes B. Fuertes,[2]* María V. Girart,[2]* Luciana L. Molinero,[3]* Carolina I. Domaica,[2]* Lucas E. Rossi,[2]* María M. Barrio,[†] José Mordoh,[†‡] Gabriel A. Rabinovich,[2]* and Norberto W. Zwirner[2,4]*

Most tumors grow in immunocompetent hosts despite expressing NKG2D ligands (NKG2DLs) such as the MHC class I chain-related genes *A* and *B* (MICA/B). However, their participation in tumor cell evasion is still not completely understood. Here we demonstrate that several human melanomas (cell lines and freshly isolated metastases) do not express MICA on the cell surface but have intracellular deposits of this NKG2DL. Susceptibility to NK cell-mediated cytotoxicity correlated with the ratio of NKG2DLs to HLA class I molecules but not with the amounts of MICA on the cell surface of tumor cells. Transfection-mediated overexpression of MICA restored cell surface expression and resulted in an increased in vitro cytotoxicity and IFN-γ secretion by human NK cells. In xenografted *nude* mice, these melanomas exhibited a delayed growth and extensive in vivo apoptosis. Retardation of tumor growth was due to NK cell-mediated antitumor activity against MICA-transfected tumors, given that this effect was not observed in NK cell-depleted mice. Also, mouse NK cells killed MICA-overexpressing melanomas in vitro. A mechanistic analysis revealed the retention of MICA in the endoplasmic reticulum, an effect that was associated with accumulation of endoH-sensitive (immature) forms of MICA, retrograde transport to the cytoplasm, and degradation by the proteasome. Our study identifies a novel strategy developed by melanoma cells to evade NK cell-mediated immune surveillance based on the intracellular sequestration of immature forms of MICA in the endoplasmic reticulum. Furthermore, this tumor immune escape strategy can be overcome by gene therapy approaches aimed at overexpressing MICA on tumor cells. ***The Journal of Immunology,*** **2008, 180: 4606–4614.**

Natural killer cells mediate cytotoxicity and IFN-γ secretion against virus-infected and tumor cells through recognition of target cells by germline-encoded activating receptors. Although some act as primary receptors for target cell recognition, others act as coreceptors. NK cell receptors act in concert to promote cytotoxicity and cytokine secretion (1). One of the most extensively studied activating NK cell receptors is NKG2D, a cell surface glycoprotein expressed on human and mouse NK cells, $\delta\gamma$ and $\alpha\beta$ $CD8^+$ T lymphocytes (2, 3). Human NKG2D ligands (NKG2DL)[5] are the MHC class I chain-related genes *A* and *B* (MICA and MICB) and the GPI-bound cell surface molecules UL16-binding protein (ULBP)-1, -2, and -3 (3, 4). In mice, NKG2DLs comprise the *retinoic acid early inducible gene* (*Rae*)*-1* family (a group of GPI-anchored, cell surface glycoproteins), the H60 molecule (an integral transmembrane protein), and the murine ULBP-like transcript 1 or MULT-1 (3, 4). Human NKG2D binds mouse NKG2DLs, and mouse NKG2D can recognize some human NKG2DLs, reflecting a selective advantage of preserving the NKG2D receptor in both species. Most NKG2DLs, in particular MICA, are almost absent in normal cells but up-regulated upon infection or neotransformation (2, 5–11).

Current evidence indicates that the MICA-NKG2D system participates in immune surveillance against tumors (3, 4, 10, 12). However, although tumors express NKG2DLs, they grow progressively in healthy individuals due to multiple tumor immune escape mechanisms (13–15), some of which affect NKG2D-dependent functions (16). Therefore, although expression of NKG2DLs on tumor cells plays a critical functional role in immune surveillance (17–20), secretion of the ectodomain of MICA dampens NK and T cell-mediated cytotoxicity due to

*Laboratorio de Inmunogenética, Hospital de Clínicas and Departamento de Microbiología, Facultad de Medicina, Universidad de Buenos Aires, Buenos Aires, Argentina; †Centro de Investigaciones Oncológicas, Fundación para la Investigación y Prevención del Cáncer, Buenos Aires, Argentina; and ‡Fundación Instituto Leloir, Buenos Aires, Argentina

Received for publication March 28, 2007. Accepted for publication January 20, 2008.

The costs of publication of this article were defrayed in part by the payment of page charges. This article must therefore be hereby marked *advertisement* in accordance with 18 U.S.C. Section 1734 solely to indicate this fact.

[1] This work was funded by grants from Agencia Nacional de Promoción Científica y Tecnológica, Consejo Nacional de Investigaciones Científicas y Técnicas de Argentina, Universidad de Buenos Aires, and Fundación Antorchas (all to N.W.Z.). M.B.F., M.V.G., and C.I.D. are postgraduate fellows of Consejo Nacional de Investigaciones Científicas y Técnicas de Argentina. L.E.R. holds a fellowship of Agencia Nacional de Promoción Científica y Tecnológica. M.M.B. is a fellow of Fundación Sales. J.M., G.A.R., and N.W.Z. are members of the Researcher Career of Consejo Nacional de Investigaciones Científicas y Técnicas de Argentina. Fundación Sales provided extra support.

[2] Current address: Laboratorio de Inmunopatología, Instituto de Biología y Medicina Experimental, Consejo de Investigaciones Científicas y Técnicas.

[3] Current address: Department of Medicine, University of Chicago, Chicago, IL.

[4] Address correspondence and reprint requests to Dr. Norberto W. Zwirner, Laboratorio de Inmunopatología., Instituto de Biología y Medicina Experimental, Vuelta de Obligado 2490, C1428ADN Buenos Aires, Argentina. E-mail address: nwz@sinectis.com.ar

[5] Abbreviations used in this paper: NKG2DL, NKG2D ligand; FC, flow cytometry; MICA/B, MHC class I chain-related gene A/B; sMICA, soluble MICA; ULBP, UL16-binding protein; ER, endoplasmic reticulum; IC, isotype-matched negative control mAb; LN, lymph node; DN, dominant negative; EGFP, enhanced GFP.

down-regulation of NKG2D on NK cells and $CD8^+$ T lymphocytes, whereas tumors that secrete MICA still express significant amounts of this NKG2DL on their cell surface (21, 22). Also, soluble MICA drives the expansion of a population of $CD4^+NKG2D^+$ T cells with immunosuppressive properties in the blood of tumor-bearing patients (23).

In this work, we investigated the occurrence of additional MICA-dependent tumor escape strategies. We found that many melanomas expressed low or undetectable levels of MICA on the cell surface but exhibited intracellular deposits of this NKG2DL, which conferred resistance to NK cell-mediated cytotoxicity. Transfection-mediated cell surface overexpression of MICA overturned this resistance and promoted in vitro cytotoxicity and IFN-γ secretion by NK cells. More importantly, overexpression of MICA delayed tumor growth in vivo and promoted apoptosis of tumor cells. Analysis of the mechanisms involved in this immune escape strategy revealed retention of MICA in the endoplasmic reticulum (ER) of melanoma cells due to accumulation of immature forms of this polypeptide. In addition, MICA was retrotransported to the cytosol and degraded by the proteasome. Our results show that retention of immature forms of MICA in the ER represents a novel tumor escape strategy that prevents NK cell-mediated cytotoxicity.

Materials and Methods

Antibodies

The following mAbs were used: anti-ULBP-1, -2, and -3 and anti-TGF-β (R&D Systems); FITC-labeled anti-EEA1, anti-LAMP2, anti-GM130, and anti-calnexin (BD Biosciences); FITC-labeled isotype-matched negative control (IC; Southern Biotech); unlabeled anti-human NKG2D 1D11 and anti-mouse NKG2D (R&D Systems); IC and PE-labeled anti-CD49b (DX5; eBioscience); panreactive anti-HLA class I mAb W6/32 (purified from hybridoma culture supernatants) and anti-HLA-E mAb MEM-06 (EXBIO); anti-actin (Santa Cruz Biotechnology); anti-calnexin TO-5 mAb (kindly provided by Dr. Soldano Ferrone (Roswell Park Cancer Institute, Buffalo, NY); and anti-MICA/B mAb D7 (24). This mAb reacts by flow cytometry (FC) with human epithelial and carcinoma cell lines. Anti-asialo-GM1 Ab was from Wako. PE-labeled goat anti-mouse IgG (DAKO), FITC-labeled mouse anti-rat IgG2b mAb (Southern Biotech), or Cy3-labeled donkey anti-mouse IgG (Jackson Immunoresearch Laboratories) were used for indirect flow cytometries or confocal microscopies.

Cell lines

The following human melanoma cell lines were used: IIB-MEL-LES (25); IIB-MEL-IAN (25); IIB-MEL-J (26); SK-MEL-28 (American Type Culture Collection; ATCC); SK-MEL-24 (ATCC); M8 (provided by Dr. M. Pérez, Autoridad Regulatoria Nuclear, Buenos Aires, Argentina) (27); MEL-888 (provided by Dr. O. Podhajcer, Instituto Leloir, Buenos Aires, Argentina); A375N (a gift from Dr. E. Medrano, Baylor College of Medicine, Houston, TX) 28); CIO-MEL-001 and CIO-MEL-002. CIO-MEL-001 is a cell line established from a metastasis of a melanoma detected in a 33-year-old white woman who after entering a phase I clinical trial remained free of disease for >30 mo. CIO-MEL-002 is a cell line established from a primary melanoma of a 27-year-old white woman. This patient was treated with IFN-α but 29 mo later developed metastases and progressive disease, and died 39 mo after the initial diagnosis (M. Barrio et al., unpublished observation). Cells were cultured in 10% FBS (NatoCor, Córdoba, Argentina) in DMEM (Sigma-Aldrich), supplemented with sodium pyruvate, glutamine, and antibiotics (all from Sigma-Aldrich).

Human melanoma samples

Tumor samples from six melanoma metastases were obtained following local institutional ethical committee guidelines by surgical excision from skin or lymph node (LN) metastases. Procedures were followed in accordance with the Declaration of Helsinki and after approval by the institutional review board. Informed consent was obtained from each patient. Samples were processed for routine histology and for preparation of cell suspensions. In this case, fat was removed with a scalpel; tumors were rinsed with fresh DMEM and cut into small pieces. For dermic metastases, a digestion for 2–16 h at 37°C with 50–100 U/ml collagenase type I (Invitrogen Life Technologies) in complete DMEM was performed. Thereafter, tissue was disrupted by passages through a sterile metal mesh to obtain a cell suspension. Cells were centrifuged, resuspended, washed with fresh medium, counted, and frozen in liquid nitrogen.

Flow cytometry

Expression of NKG2DLs was analyzed by FC with specific mAbs and PE-labeled anti-mouse IgG (DAKO) in a FACSCalibur flow cytometer (BD Biosciences). In some experiments, the specific fluorescence index was calculated as the mean fluorescence produced by each mAb divided by the mean fluorescence produced by the IC mAb. In other experiments, the ABC parameter (number of Ab molecules bound per cell) was calculated calibrating the flow cytometer with Quantibrite particles (BD Biosciences). In some experiments, melanoma cells were cultured for 24 h with or without 50 nM proteasome inhibitor bortezomib (Velcade), and surface MICA expression was assessed by FC.

SDS-PAGE and Western blot

SDS-PAGE and Western blot were performed as described, using anti-MICA polyclonal Ab (6, 29), the anti-calnexin mAb TO-5, or anti-actin Ab. Bound Abs were detected using HRP-labeled anti-rabbit or anti-mouse IgG (Bio-Rad) and chemiluminescence. No bands were observed in Western blots incubated with normal rabbit IgG. For experiments with endoH, MICA was detected with biotinylated anti-MICA Abs and HRP-labeled streptavidin (Southern Biotech).

NK cells

Human NK cells were isolated from blood of healthy donors using the RosetteSep NK cell enrichment kit (Stem Cell). Mouse NK cells were isolated from spleens of nude mice using the SpinSep mouse NK cell enrichment kit (Stem Cell).

Cytotoxicity

Five-hour standard ^{51}Cr release assays were performed using 5000 target melanoma cells/well and NK cells as effector cells. The percent of cytotoxicity was calculated as $100 \times [(cpm_{exp} - cpm_{sp})/(cpm_{max} - cpm_{sp})]$ (in which cpm_{max} is maximum release, obtained from target cells lysed with 2% Triton X-100, cpm_{exp} is release of the particular experimental condition, and cpm_{sp} is the spontaneous release). In some experiments, cytotoxicity was performed in the presence of the blocking anti-NKG2D mAb 1D11 or an IC mAb at 10 μg/ml.

Indirect immunofluorescence

Cells were fixed with 2% paraformaldehyde and incubated with 200 μg/ml D7 or the IC mAbs for 30 min. Bound Ab were detected with Cy3-labeled donkey anti-mouse IgG. Slides were mounted with 1,4-diazabicyclo[2.2.2]octane and observed in a digital Eclipse E800 Nikon C1 confocal microscope. For immunofluorescence with permeabilization, cells were treated with 0.1% saponin for 10 min after fixing. Staining procedures were performed as described, but 0.1% saponin was included in the solutions. For colocalization experiments, fixed and permeabilized cells were incubated with the mAb D7 and Cy3-labeled donkey anti-mouse IgG, washed, and incubated with FITC-labeled anti-EEA1, anti-GM130, anti-LAMP2, or anti-calnexin mAbs. Paraffin-embedded sections were used for colocalization of MICA with calnexin in melanoma metastases.

Electronic microscopy

IIB-MEL-LES cells were fixed with 4% paraformaldehyde and 0.75% glutaraldehyde, harvested, washed, and dehydrated with ethanol. Cells were embedded in acrylic resin and benzoyl peroxide. Ultrathin sections were used for immunostaining with the mAb D7 and goat anti-mouse IgG conjugated to 10-nm-diameter colloidal gold particles (Sigma-Aldrich). Samples were counterlabeled with 1% uranyl acetate and Reynolds solution and observed in a C10 Zeiss Electron Microscope. Microphotographs were obtained on Kodak 4489 films.

Transfections

Full-length MICA*001 was cloned into pCIneo from cDNA obtained from the HCT116 cell line. Absence of mutations was checked by DNA sequencing. IIB-MEL-LES melanoma cells were stably transfected with pCIneo-MICA or empty plasmid using Lipofectamine 2000 (Invitrogen Life Technologies). Stably transfected cells were selected for cell surface MICA expression (assessed by FC) and cloned. Three clones that stably express MICA on their cell surface (clones 1, 2, and 3) and one clone transfected with empty plasmid (clone C) were generated and further cultured with G418. In vitro proliferation of clones and the parental cell line

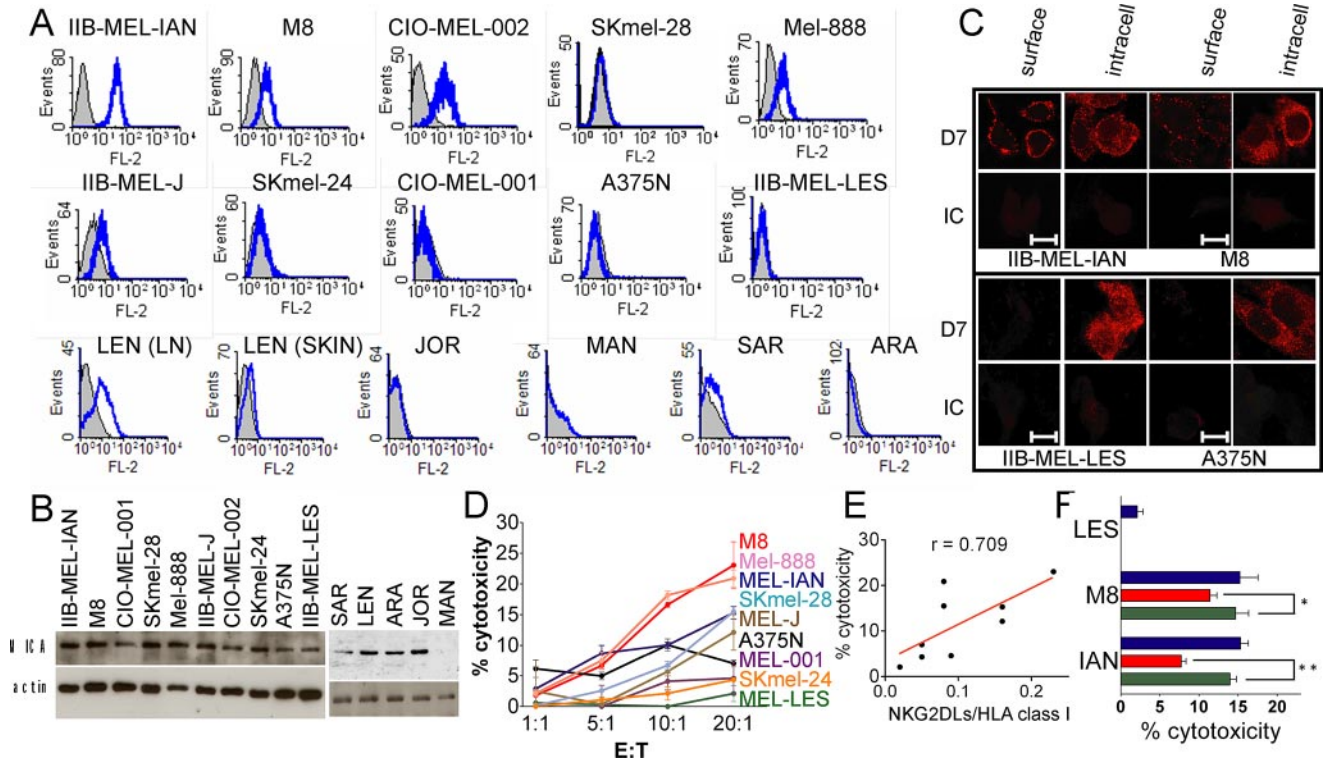

FIGURE 1. Expression of MICA/B by human melanomas and susceptibility to NK cell-mediated lysis. *A* and *B*, Expression of MICA/B (blue histograms) by 10 human melanoma cell lines and melanoma metastases from five patients was analyzed by FC (*A*) or Western blot (*B*). *A*, Filled histograms: IC mAb. *B*, Western blots were normalized against β-actin. *C,* Immunofluorescence on fixed (surface) or fixed and permeabilized (intracell) melanoma cells and confocal microscopy. Bar = 10 μm. *D*, Cytotoxicity of human NK cells at different E:T ratios against nine human melanoma cell lines (names indicated on the right) as target cells. *E*, Correlation between cytotoxicity and the ratio of NKG2DL to HLA class I expression in different melanoma cell lines. *F*, Cytotoxicity was also assessed in the absence (blue bars) or presence of a blocking anti-NKG2D mAb (red bars) or an IC mAb (green bars) using NK cells and the indicated cell lines. E:T = 20:1. Values are means $\pm$ SD. *, $p < 0.05$; **, $p < 0.01$. Results are representative of three independent experiments.

was assessed by the 3-(4,5-dimethylthiazol-2-yl)-5-(3-carboxymethoxyphenyl)-2-(4-sulfophenyl)-2*H*-tetrazolium inner salt (MTS) assay the (CellTiter 96 AQueous Assay; Promega). In other experiments, IIB-MEL-LES cells were transiently transfected with the bicistronic pMSCV2.2 plasmid encoding wild-type or dominant-negative (DN) p97 protein and enhanced GFP (EGFP) (provided by Dr. Peter Cresswell, Yale University, New Haven, CT), which allows the correlation of EGFP and p97 expression (30). Melanoma cells were transfected with Lipofectamine 2000, cultured for 24 h, and analyzed for surface MICA expression in the $EGFP^+$ and $EGFP^-$ cell populations.

In vivo tumor challenge

Experiments with mice were performed with approval of the local ethical committee, and according to National Institutes of Health guidelines (Guide for Care and Use of Laboratory Animals). Groups of four to six female Swiss N:NIH(S)nu (*nude*) mice 6–7 wk old were injected s.c. in the right flank with transfected cells (5×10^6 cells). Tumor growth was measured every 2–3 days using a caliper. Tumor volume was calculated as $(d^2 \times l)/2$, where d and l are the minor and major diameters, respectively. Mice were sacrificed when tumors reached 2 cm^3. Mice with tumor volume <0.5 cm^3 were considered tumor free. Tumors were recovered from sacrificed animals, and surface MICA expression was assessed. Also, spleen cell suspensions were frozen in liquid nitrogen and later processed for assessment of NKG2D expression on NK cells ($DX5^+$ cells) by FC. In other experiments, tumor-bearing mice were sacrificed at day 48, tumors were excised, frozen in liquid nitrogen, and used for assessment of apoptosis in vivo on 10-μm-thick tumor cryosections by TUNEL using the ApopTag fluorescein in vivo apoptosis detection kit (Chemicon) and confocal microscopy. For NK cell depletion, mice received 20 μg of the anti-asialo GM1 Ab per mouse on days -1, 7, 17, 31, and 42 by i.p. injection. Control mice received equivalent amounts of normal rabbit IgG the same days.

ELISA

A capture ELISA was developed to detect soluble MICA (sMICA) using the D7 mAb coated onto Maxisorp plates (NUNC) and recombinant sMICA as standard. For sMICA detection, culture supernatants were concentrated 50 times in Centricon tubes (Millipore). Captured MICA was detected using rabbit anti-MICA serum 621 (6), HRP-labeled goat anti-rabbit IgG, and *o*-phenylenediamine (Sigma-Aldrich).

Secretion of TGF-β or IFN-γ was analyzed by capture ELISA, using a paired set of anti-TGF-β mAbs (R&D Systems) or anti-IFN-γ mAbs (Pierce Chemical Co.) and peroxidase-labeled streptavidin (Pierce Chemical Co.). Acidified culture supernatants were used to detect bioactive TGF-β. Standard curves were obtained using rTGF-β or rIFN-γ.

Sequencing of MICA

Total RNA from the melanoma cell lines was extracted using Trizol (Invitrogen Life Technologies), and MICA cDNA (obtained with the Advantage RT-for-PCR kit from Clontech) was sequenced as described (29). Raw sequences were compared with published sequences using the CLUSTALW alignment program (www.ebi.ac.uk/clustalw/) and further inspected manually.

EndoH digestions

Twenty micrograms of proteins from melanoma cell lysates were digested with 1500 U of endoH (New England Biolabs) during 4 h at 37°C. MICA expression was thereafter analyzed by Western blot. Films were scanned and analyzed with the Scion Image analysis software (www.scioncorp.com). The mean intensity of each band was recorded and used for the calculation of the percentage of digested and undigested forms of MICA.

Cell fractionation

Cells were cultured for 24 h with or without 50 nM proteasome inhibitor bortezomib, and membrane and cytosolic fractions were obtained by mechanic disruption of cell suspensions in TBS with protease inhibitors, centrifugation at 1,000 $\times$ *g* for 10 min, and ultracentrifugation (100,000 $\times$ *g* for 60 min at 4°C). The supernatant (cytosolic fraction) was collected and stored; the pellet was resuspended in TBS supplemented with 1% CHAPS and protease inhibitors, ultracentrifuged at 100,000 $\times$ *g* for 60 min at 4°C,

Table I. *NKG2DL, HLA class I, and HLA-E expression, and MICA genotyping of the 10 human melanoma-derived cell lines used in this study*[a]

Rank	Cell	MICA/B	ULBP-1	ULBP-2	ULBP-3	HLA Class I	HLA-E	MICA Typing
1	M8	718.65 ± 297.35	1359.90 ± 137.26	13449.29 ± 9.80	741.53 ± 84.57	71938.07 ± 518.75	24714.23 ± 2651.89	MICA*008/MICA*008
2	IIB-MEL-J	673.33 ± 99.31	482.05 ± 38.02	4958.39 ± 669.49	886.27 ± 6.02	44056.25 ± 3132.40	302.43 ± 3.28	MICA*001/MICA*008
3	IIB-MEL-IAN	2294.47 ± 13.92	94.04 ± 34.83	3062.10 ± 645.40	1070.43 ± 66.85	40914.26 ± 3767.15	424.75 ± 50.52	MICA*001/MICA*001
4	A375N	63.31 ± 29.42	15.66 ± 8.04	2269.28 ± 35.93	163.32 ± 44.37	51778.22 ± 4001.77	2871.18 ± 294.93	MICA*004/MICA*044
5	CIO-MEL-002	845.37 ± 38.59	260.19 ± 38.07	388.14 ± 44.32	573.73 ± 54.31	12690.20 ± 1308.17	316.04 ± 35.89	MICA*005/MICA*011
6	Skmel-24	375.75 ± 55.15	21.37 ± 27.70	1299.76 ± 109.55	31.99 ± 16.55	31716.84 ± 7923.77	3541.74 ± 418.18	MICA*008/MICA*027
7	CIO-MEL-001	239.50 ± 58.98	74.03 ± 42.85	1266.14 ± 122.16	77.94 ± 46.76	18032.17 ± 4083.10	180.35 ± 55.65	MICA*001/MICA*001
8	Skmel-28	185.91 ± 10.71	9.42 ± 6.20	1275.24 ± 36.35	168.38 ± 63.16	26947.82 ± 7327.31	1618.62 ± 156.89	MICA*008/MICA*008
9	Mel-888	718.82 ± 24.31	82.88 ± 45.27	310.32 ± 95.5	345.76 ± 176.1	17800 ± 3421.35	1079.34 ± 229.62	MICA*009/MICA*009
10	IIB-MEL-LES	149.15 ± 109.42	82.04 ± 3.74	633.91 ± 11.16	307.73 ± 32.52	71671.59 ± 2554.71	1242.66 ± 127.24	MICA*001/MICA*011

[a] Underlined cells did not express or expressed very low amounts of MICA on the cell surface. MICA expression was assessed by FC, and values correspond to the ABC ± SEM calculated as explained in *Materials and Methods*. Cell lines were ranked according to the total amount of NKG2DLs (sum of ABC values of MICA/B and ULBPs).

FIGURE 2. Restoration of cell surface expression of MICA and functional consequences in vitro. *A,* Expression of MICA on the cell surface of clones of stably transfected IIB-MEL-LES cells. Clone C (thin line): clone transfected with empty plasmid; clones 1–3: clones transfected with full length MICA (thick, dotted and dashed lines, respectively). Filled histogram: IC mAb. *B,* Cytotoxicity of human NK cells against MICA-transfected clones 1–3 (●, □, and ○, respectively), the control clone C (∗), and the parental IIB-MEL-LES cells (♦). *C,* IFN-γ secretion by NK cells upon coculture with the transfected clone 1 (●). □, Clone C; ■, parental cells IIB-MEL-LES. Clones 2 and 3 produced results similar to those of clone 1 (not shown). *D,* Cytotoxicity of human NK cells against clones 1–3 and clone C in the absence (□) or presence of the blocking anti-NKG2D mAb 1D11 (▨) or an IC mAb (■) at E:T = 20:1. *E,* IFN-γ secretion of human NK cells upon coculture with clone 1 or clone C (same bar pattern as in *D*). **, $p < 0.01$ vs clone C (in *B* and *C*) or IC (in *D* and *E*). *F,* In vitro proliferation of MICA-transfected clones 1–3, the control clone C, and the parental cell lines IIB-MEL-LES assessed by the microtubule binding protein spin-down assay. Values in *B–F* are means ± SD. Experiments were repeated three times with similar results.

and the resulting supernatant was collected and stored (membrane fraction). MICA expression was assessed by Western blot. Lack of cross-contamination between fractions was assessed by Western blot analysis of HLA class I using the HC10 mAb and heat shock protein 70 using the BRM-22 mAb (Sigma-Aldrich).

Protein concentration in each fraction was assessed by the Micro BCA method (Pierce Chemical Co.).

Statistical analyses of data

ANOVA with Dunnett's comparison test was used to compare cytotoxicity, IFN-γ secretion, tumor growth, and NKG2D expression. An unpaired *t* test was used to compare the levels of endoH-digested MICA. The Pearson's test was used to analyze the correlation between two independent parameters (cytotoxicity, cell surface MICA, HLA class I, or MICA/HLA class I). Results are presented as mean ± SD or SEM.

Results

Low cell surface expression of NKG2DLs on melanomas prevents NK cell-mediated cytotoxicity

We first investigated cell surface expression of NKG2DLs on 10 melanoma cell lines and the expression of MICA/B on 6 melanoma metastases from skin or LNs. As shown in Fig. 1*A*, 5 of 10 cell lines and 3 of 6 metastasis-derived cells did not express or expressed very low amounts of MICA/B on the cell surface. In one case (LEN), analysis of two metastases showed higher expression of MICA/B on LN-derived than on skin-derived melanoma cells. FC analysis of NKG2DLs confirmed these data and revealed that IIB-MEL-LES and A375N cells expressed the lowest amounts of MICA whereas IIB-MEL-IAN expressed the highest amount of this protein (Table I). A wider phenotypic characterization of other NK cell receptor ligands revealed that expression of ULBPs-1, -2, and -3 was heterogeneous while all cell lines expressed high amounts of HLA class

I molecules and diverse amounts of HLA-E (Table I). By Western blot analysis, we observed that all cell lines and four metastases showed MICA expression (Fig. 1*B*), which was confirmed by immunofluorescence staining on cells that were positive (IIB-MEL-IAN and M8) or negative (IIB-MEL-LES and A375N) for cell surface MICA expression (Fig. 1*C*). In one metastasis (MAN), we did not detect MICA expression. No correlation between cell surface expression of MICA and total amounts of MICA was observed, as judged by comparative analysis of flow cytometry and Western blots after normalization against β-actin ($r = 0.439$; not shown). Interestingly, melanoma cell lines exhibited different susceptibility to NK cell-mediated cytotoxicity (Fig. 1*D*) which correlated with the ratio of total NKG2DL to HLA class I expression (Fig. 1*E*; $r = 0.709$) but not with cell surface expression of MICA, NKG2DL, or HLA class I molecules. Remarkably, IIB-MEL-LES and A375N were resistant to NK cell-mediated cytotoxicity (Fig. 1*D*), and lysis of M8 and IIB-MEL-IAN was partially dependent of NKG2D (Fig. 1*F*). Thus, intracellular retention of MICA confers resistance to NKG2D-dependent NK cell mediated-cytotoxicity in vitro.

Restoration of cell surface MICA delays in vivo tumor growth and promotes NK cell-mediated tumor cell apoptosis

By transfection of IIB-MEL-LES cells with full-length *MICA* cDNA, we induced cell surface expression and generated three stably transfected clones (Fig. 2*A*) that showed susceptibility to NK cell-mediated lysis (Fig. 2*B*) and promoted IFN-γ secretion (Fig. 2*C*). Blockade with an anti-NKG2D mAb confirmed that overexpression of MICA was responsible for this susceptibility (Fig. 2*D*) and enhanced IFN-γ secretion (Fig. 2*E*). Because the transfection did not modify the expression of UBLPs1–3 or HLA-E (not shown), we ruled out the possibility that the enhanced NK cell-mediated functions could be due to up-regulation of other NKG2DLs or of the ligand of CD94/NKG2C. All transfected clones exhibited similar growth in vitro (Fig. 2*F*), indicating that MICA overexpression did not alter the intrinsic growth properties of melanoma cells.

To investigate the impact of these findings in tumor-immune escape in vivo, we challenged *nude* mice with MICA- or mock-transfected melanoma clones. Mice injected with mock-transfected cells (clone C) developed progressively growing tumors and terminal morbidity by 40–45 days after challenge. Conversely, terminal morbidity was reached at days 63–73 for clone 1, at days 55–60 for clone 2, and at days 66–75 for clone 3, and the differences in tumor growth were statistically significant (Fig. 3*A*). All animals that received tumors overexpressing MICA remained tumor free at a time at which ~50% of control animals developed tumor (~day 50). Also, only 50% of mice that received clones overexpressing MICA developed tumors at a time at which 100% of control mice developed tumors (~day 67; Fig. 3*B*). Remarkably, tumors recovered from the mice challenged with clones 1 to 3 stably conserved surface expression of MICA (Fig. 3*C*). TUNEL assays on cryosections of tumors from mice challenged with melanoma cells overexpressing MICA sacrificed at day 48 showed extensive tumor cell apoptosis (Fig. 3*D*), whereas NK cells from *nude* mice lysed MICA-overexpressing cells in vitro more efficiently than the mock-transfected cells (Fig. 3*E*). In addition, tumor growth of MICA overexpressing melanomas in NK cell-depleted mice was identical with the growth of control tumor cells in NK cell-sufficient mice (Fig. 3*A*), confirming that NK cells are the main effector cells that control tumor growth in vivo in this experimental setting. Because ~2 mo after inoculation, MICA-overexpressing tumors reached the same penetrance compared with control tumors, we assessed whether MICA-overexpressing tumors might promote systemic down-regulation of NKG2D that could impair the immune response mediated by NK

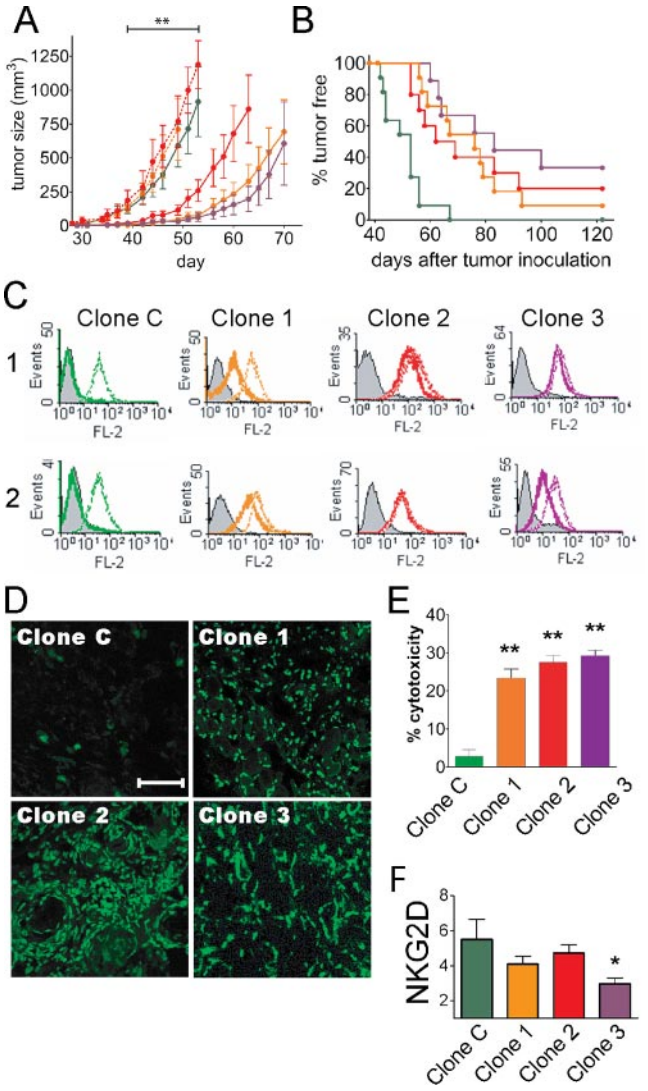

FIGURE 3. Overexpression of MICA in melanoma cells overcomes tumor cell resistance and promotes NK cell-mediated tumor rejection in vivo. *A,* In vivo growth of clones 1–3 (continuous orange, red, and purple lines, respectively) or clone C (green line) in NK cell-sufficient *nude* mice or in NK cell-deficient *nude* mice (clone 1, dashed orange line; clone 2, dashed red line). NK cell-deficient *nude* mice were produced by repeated injection of anti-asialo-GM1 Ab. *nude* mice were inoculated s.c. with 5×10^6 cells of the different clones on day 0, and tumor growth was assessed as explained in *Materials and Methods*. Each tumor clone injected in control mice that received normal rabbit IgG instead of anti-asialo-GM1 Ab showed a growth identical with that in mice that did not receive any treatment (and therefore were not depicted). *B,* Tumor-free animals (Kaplan-Meier analysis, same color pattern as in *A*). *C,* Cell surface MICA (continuous lines) and HLA class I molecules (dotted lines) on tumors recovered from mice at the time of euthanasia. Filled histograms: IC mAb. Results of two representative animals (1 and 2) of each group are shown. *D,* In vivo apoptosis of the human melanomas on cryosections of the tumor areas, assessed by TUNEL assay and confocal microscopy. Bar = 50 μm. *E,* Cytotoxicity of mouse NK cells against clones 1–3 and clone C (same color pattern as in *A,* assessed at E:T ratio = 50:1. Mean ± SD are shown in *A* and *E*. **, $p < 0.01$ vs clone C. *F,* Expression of NKG2D (specific fluorescence index) on spleen NK cells (defined by gating on DX5$^+$ cells) recovered from nude mice that received the different tumor clones (indicated on the *x*-axis) at the time of euthanasia of each animal. Values are means ± SEM. *, $p < 0.05$ vs clone C. Experiments were repeated three times yielding similar results.

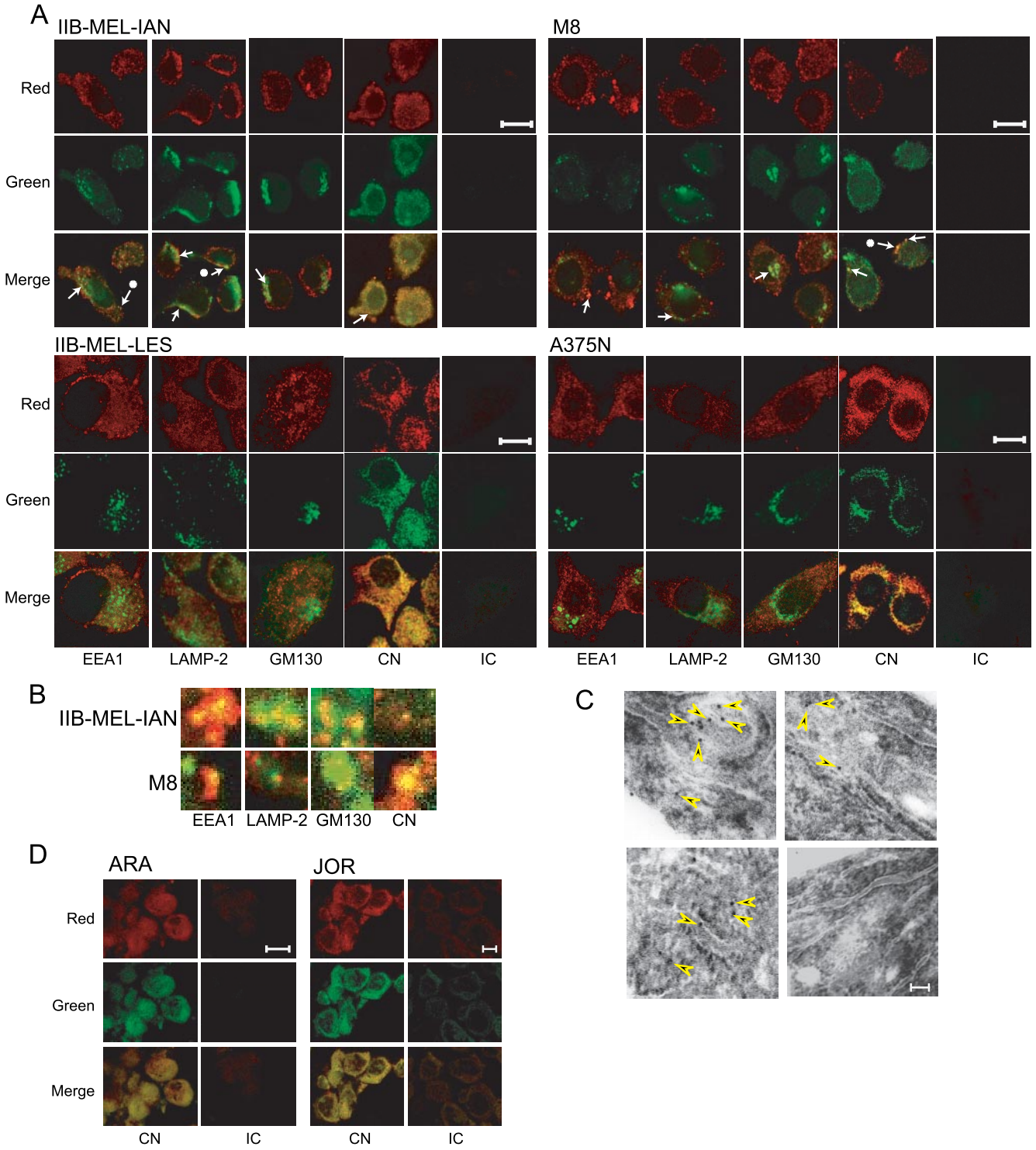

FIGURE 4. Subcellular localization of MICA in human melanoma cells. *A*, MICA was detected with the mAb D7 and Cy3-labeled secondary Ab (red) in the indicated cell lines. Colocalization markers were detected using FITC-labeled mAbs specific for EEA1 (early endosomes), LAMP-2 (late endosomes/lysosomes), GM130 (Golgi) and calnexin (CN, ER). Analysis was performed by confocal microscopy. White arrows show colocalization (yellow staining) in IIB-MEL-IAN and M8 cells. IC: isotype control mAb. Bar = 10 μm. *B*, Higher magnification of indicated areas of *A*. *C*, Electronic microscopy of IIB-MEL-LES cells stained with the mAb D7 (*top* and *bottom* left images) or an IC mAb (*bottom right* image). Arrowheads, MICA localized in association with ER cisternae. Bar = 100 nm. Results are representative of three independent experiments. *D*, Colocalization of MICA and CN assessed by confocal microscopy in paraffin-embedded sections of melanoma metastases. Bar = 10 μm.

cells. In fact, spleen-derived NK cells of mice challenged with MICA-overexpressing tumors collected at the time of the euthanasia expressed visibly lower levels of NKG2D compared with spleen-derived NK cells of mice challenged with control tumors (Fig. 3*F*; $p < 0.05$ for clone 3; NS for clones 1 and 2). Hence, restoration of cell surface expression of MICA by gene transfer confers susceptibility to NK cell-mediated apoptosis which delays in vivo growth of melanoma cells, indicating that tumor immune escape mechanisms based on intracellular retention of MICA can be successfully overcome to promote NKG2D-dependent NK cell-mediated cytotoxicity.

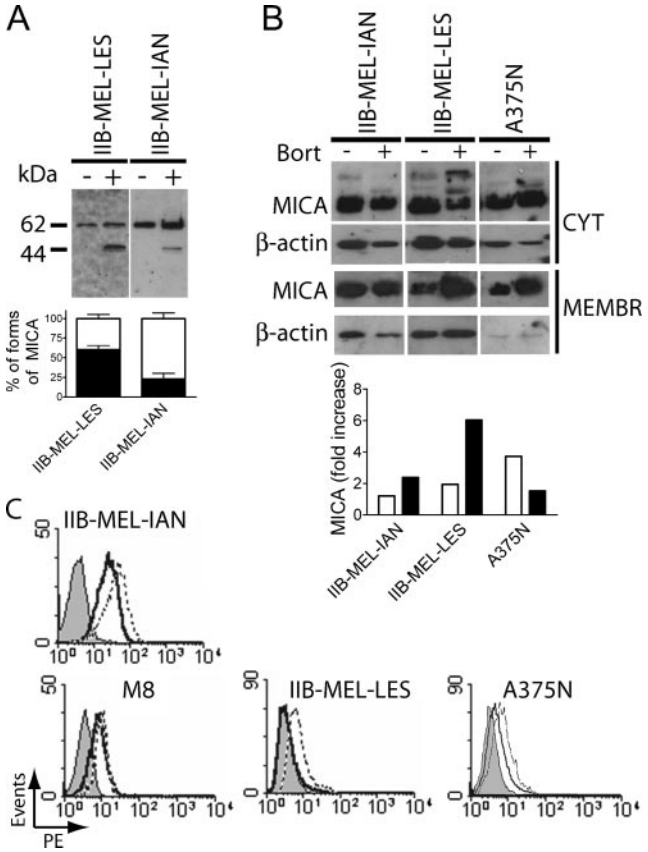

FIGURE 5. EndoH-sensitivity, transport to the cytoplasm, and degradation by the proteasome accounts for the lack of cell surface expression of MICA in human melanoma cells. *A*, Western blot analysis of MICA in cell lysates of IIB-MEL-LES and IIB-MEL-IAN cells untreated (−) or treated (+) with endoH as described in *Materials and Methods*. *Top,* Representative Western blot analysis showing the undigested form of $M_r \sim 62$ kDa and a digested form of $M_r \sim 44$ kDa of MICA in the presence of the enzyme. *Bottom,* Mean percentage of undigested (□) and digested (■) forms of MICA in both cell lines from three independent experiments. For calculations, Western blot membranes were scanned and analyzed with the Scion Image software analysis as explained in *Materials and Methods*. The mean ± SEM is shown. $p = 0.0162$ ($n = 3$) for digested form of MICA in IIB-MEL-LES vs digested form of MICA in IIB-MEL-IAN. *B*, Western blot analysis of MICA and actin in cytosolic (CYT) and membrane (MEMBR) fractions of IIB-MEL-IAN, IIB-MEL-LES and A375N cells untreated (−) or treated (+) with the proteasome inhibitor bortezomib (Bort). *Bottom,* Analysis of the intensity of MICA in cytosolic (□) and membrane fractions (■). Fold increase was calculated as [intensity of the band of MICA/intensity of the band of actin]$_{\text{with bortezomib}}$/[intensity of the band of MICA/intensity of the band of actin]$_{\text{without bortezomib}}$. *C,* Cell surface expression of MICA (assessed by FC) in the indicated cell lines untreated (thick line) or treated with bortezomib (thin line).

Intracellular compartmentalization of MICA in human melanoma cells

To gain insight into the mechanistic basis underlying the absence of MICA on the surface of melanoma cells, we first explored secretion of soluble MICA in melanoma cell-conditioned medium. Under our experimental conditions and detectability of our ELISA assays, we could detect no sMICA in culture cell supernatants (not shown). Also, cell surface expression of MICA was not observed when melanomas were cultured with cytochalasin B or chloroquine, indicating that a fast turnover did not account for low cell surface expression. Remarkably, none of the cell lines used secreted detectable TGF-β, and incubation with a neutralizing anti-TGF-β mAb for up to 48 h was not capable of restoring cell surface MICA expression (not shown), as has been previously shown (31).

Next, the subcellular localization of MICA was investigated by colocalization experiments and confocal microscopy (Fig. 4*A, B*). In IIB-MEL-IAN and M8 cells, we detected MICA in endosomes (EEA1), lysosomes (LAMP-2), Golgi apparatus (GM130), and the ER (calnexin). However, in IIB-MEL-LES and A375N cells, intracellular deposits of MICA were confined to the ER (colocalization with calnexin). This result was confirmed by immunoelectron microscopy (gold particles that labeled MICA were detected in association with the ER cisternae; Fig. 4*C*). In addition, colocalization of MICA with calnexin was also observed in two melanoma metastases that were negative for cell surface expression of MICA (Fig. 4*D*).

To determine whether point mutations or allele association could be responsible of abnormal intracellular retention of MICA, we sequenced the *MICA* mRNA derived from the 10 melanoma cell lines. As shown in Table I, we could not find point mutations or allele associations with cell surface expression of MICA in the melanoma cell lines tested.

To address whether MICA retention in the ER was associated with accumulation of immature forms of MICA, we performed endoH digestions of cell lysates of IIB-MEL-LES (cells that retain MICA in the ER) and IIB-MEL-IAN (cells that express MICA on the cell surface). IIB-MEL-LES showed a marked increase in the ratio of endoH-sensitive forms (immature molecules) vs endoH-resistant forms (mature molecules) of MICA when compared with IIB-MEL-IAN (Fig. 5*A*), indicating that MICA transited through the Golgi and acquired resistance to endoH digestion (maturation) in IIB-MEL-IAN cells but not in IIB-MEL-LES cells. Also, MICA was found in the cytoplasm and membrane fractions of IIB-MEL-LES, A375N, and IIB-MEL-IAN cells (Fig. 5*B*), although culture with the proteasome inhibitor bortezomib induced accumulation of this NKG2DL mainly in IIB-MEL-LES and A375N cells. Accordingly, cell surface expression of MICA was induced by bortezomib in melanoma cells which did not express this NKG2DL on their cell surface (IIB-MEL-LES and A375N), although it had a barely detectable effect on IIB-MEL-IAN and M8 cells (Fig. 5*C*). Interestingly, the retrotranslocation of MICA from the ER to the cytosol did not apparently involve the Sec61 channel as transient transfection of IIB-MEL-LES and IIB-MEL-IAN cells with a bicistronic plasmid encoding EGFP and p97 (a regulator of Sec61) or its DN form, DN p97 (30), did not lead to increased expression of MICA on the cell surface of EGFP$^+$ cells transfected with the plasmid encoding WT p97 compared with cells transfected with the plasmid encoding DN p97 or EGFP$^-$ cells (not transfected; not shown).

Discussion

Here we investigated cell surface expression of NKG2DLs on human melanomas and found that some cell lines and metastases do not express MICA on the cell surface but still store an intracellular pool of this NKG2DL. Expression of MICA was also observed in one primary melanoma but not on benign nevi (M. B. Fuertes, unpublished observations). A careful phenotypical evaluation showed a substantial heterogeneity in the expression of other NKG2DLs (ULBP-1, -2, and -3) and of classical and nonclassical (HLA-E) HLA molecules by the melanoma cell lines. NK cell-mediated cytotoxicity against them correlated with the ratio of NKG2DL to HLA class I molecules, but not with the overall amounts of NKG2DL or MICA, thus confirming the tight regulation of NK cell-mediated cytotoxicity upon engagement of activation and inhibitory receptors (2–5, 16). Melanomas with low NKG2DL:HLA ratio such as IIB-MEL-LES and A375N were highly resistant to NK cell-mediated lysis due to lack of expression

of MICA on the cell surface despite the existence of intracellular deposits of this NKG2DL. Therefore, we hypothesized that intracellular retention of MICA may constitute a novel mechanisms by which tumor cells evade NK cell-mediated cytotoxicity. Remarkably, under our experimental conditions, proteolytic shedding of MICA (21, 22) or TGF-β-mediated modulation (31) did not seem to be involved in down-regulation of MICA from the cell surface, suggesting that an alternative mechanism might contribute to this effect. The lack of correlation between the in vitro susceptibility to NK cell-mediated cytotoxicity and expression of NKG2DLs could also be due to the fact that some melanomas may express low amounts of ligands for other NK cell-activating receptors different from NKG2D.

Notably, transfection-mediated expression of MICA in IIB-MEL-LES cells restored its cell surface expression and triggered NKG2D-dependent NK cell-mediated cytotoxicity and induced IFN-γ secretion. This effect was directly mediated by MICA and was not due to up-regulation of ULBPs or HLA-E as a consequence of the transfection procedure, which might potentially provide a MICA-derived peptide that may stabilize HLA-E and allow recognition by CD94/NKG2C. Strikingly, successful surface expression of MICA*001 on IIB-MEL-LES cells by transfection indicates that one of its endogenous alleles can be efficiently expressed on the cell surface by ectopic gene transfer, bypassing the inherent ability of this cell to retain MICA inside the cell. This observation is compatible with the existence of a chaperone that could be involved in intracellular retention, which would probably become saturated when MICA is overexpressed using a plasmid that drives expression of this NKG2DL under the control of the SV40 promoter. This situation would be comparable with that described for Erd2, a receptor that retains KDEL sequence-carrying proteins in the ER until it becomes saturated (32).

In vivo, MICA overexpressing clones exhibited NK cell-dependent delayed growth and increased apoptosis, and this effect was mirrored by in vitro cytotoxicity mediated by mouse NK cells. These results indicate that mouse NKG2D recognizes human MICA, as has been demonstrated (20). Overexpression of MICA has been shown to delay the growth of gliomas in *nude* mice but in those experiments, outgrowing tumors lost MICA expression most likely due to in vivo selection because such tumors were not cloned (12). In our experimental setting, we observed that clones stably conserved cell surface expression of MICA at stages of tumor outgrowth. Although results obtained with clones should be interpreted cautiously, tumors overexpressing MICA appear to overcome NK cell-mediated effector mechanisms most likely by exploiting other tumor-immune escape mechanisms (13–16). For example, metalloprotease-induced shedding of sMICA which promotes systemic down-regulation of NKG2D has been shown to contribute to escape of certain tumors (21, 22). We observed systemic down-regulation of NKG2D in spleen-derived NK cells from mice challenged with tumors that overexpressed MICA, which presumably could be due to the release of sMICA. Also, tumor outgrowth of MICA-overexpressing vs control tumors observed in our experimental setting could be due to the absence of a T cell-mediated immune response because our experiments were performed in *nude* mice. Hence, up-regulation of MICA expression on tumor cells by ectopic gene transfer may be an efficient approach to trigger a NK-cell mediated response which is sufficient to control early tumor growth in vivo, even for tumors that developed a machinery to retain this NKG2DL inside the cell.

Here we demonstrated that MICA was retained in the ER but not due to point mutations that might have generated ER retention sequences such as the KDEL, KEDL, or related motifs for ER retention (32–36). In addition, none of the cells used in our experiments expressed the unstable MICA*010 protein (37). Conversely, they encoded alleles expressed at high levels on the cell surface of other cells (22, 24, 38, 39 and M. B. Fuertes, unpublished observations), confirming that retention in the ER was not due to intrinsic features of the MICA polypeptide. The detected M_r of MICA was similar in all melanomas, which suggests that oligosaccharide addition to the polypeptide takes place mainly in the ER (40). A retrograde transport of MICA from the Golgi to the ER seems unlikely because we could not detect colocalization with the *cis*-Golgi marker GM130 in IIB-MEL-LES and A375N cells. Conversely, in IIB-MEL-IAN and M8 melanoma cells, we observed localization of MICA in the Golgi apparatus, and late and early endosomes, reflecting the pool molecules in transit to the cell surface. Retention of MICA in the ER was further supported by endoH-sensitivity experiments because we observed substantial accumulation of immature forms of the MICA polypeptide in IIB-MEL-LES compared with IIB-MEL-IAN cells. In addition, MICA was translocated to the cytosol and degraded in the proteasome mainly in IIB-MEL-LES and A375N cells, whereas inhibition of the proteasome promoted accumulation and cell surface up-regulation of MICA.

Although intracellular retention of MICB, ULBP-1, and ULBP-2 in the ER and *cis*-Golgi has been described in fibroblasts infected with human CMV (41, 42), no similar phenomena have been previously described in tumor cells. Such MICA^{dull} tumor phenotype may arise during in vivo tumor growth and sculpting (13). Moreover, the restoration of cell surface expression of MICA by bortezomib suggests that chemotherapy strategies using this compound may indirectly promote up-regulation of MICA in tumors that retain this NKG2DL in the ER and foster NKG2D-dependent NK cell-mediated antitumor activity.

Retention of immature forms of MICA in the ER could be due to association to chaperones, posttranslational modifications induced by ER quality control machineries such as the unfolded protein response and the ER-associated degradation (43) or to an altered redox state that may affect protein stability within the ER (44). In fact, MICA associates with specific chaperones such as ERp5, which participates in the cleavage of this NKG2DL from the cell surface of tumor cells (45).

Intracellular retention of MICA may provide a selective advantage under immunological pressure to favor the outgrowth of tumor variants that resist NK cell-mediated functions. Such a mechanism of tumor-immune escape would not rely on metalloprotease secretion. Although it has been suggested that down-regulation of NKG2DL could contribute to tumor escape (46, 47), the fate and subcellular localization of the NKG2DLs and the involved mechanisms remain elusive. Intracellular retention of MICA may also compromise the generation and function of Ab against MICA upon specific immunotherapy, which have been shown to have prognostic value in cancer patients (48).

In summary, we provide the first evidence of a novel unrecognized tumor-immune escape strategy based on the accumulation of immature forms of MICA in the ER, retrotranslocation to the cytosol and proteasome-mediated degradation. This mechanism prevented tumor cell destruction and IFN-γ secretion by NK cells and conferred immune privilege to melanoma cells. This mechanisms could be overcome by transfection-mediated gene transfer, which restored cell surface expression of MICA, promoted NK cell-mediated cytotoxicity and conferred in vivo susceptibility to apoptosis, thus contributing to delay of tumor growth in vivo. Although we used a episomal vector for overexpression of MICA, our work constitutes a step forward in the efforts of translating NKG2DL gene transfer approaches (e.g., through adenoviral-mediated gene transfer or DNA vaccines carrying the MICA gene; Ref. 19) for the treatment of human cancer. These approaches may also be useful

for tumors that devised strategies to prevent cell surface expression of MICA due to retention in the ER.

Acknowledgments

We thank Dr. M. del R. Pérez and O. Podhajcer for providing melanoma cell lines; Dr. S. Ferrone (Roswell Park Cancer Institute, Buffalo, NY) for providing the anti-calnexin mAb, Dr. Peter Cresswell (Yale University, New Haven, CT) for providing the plasmids encoding p97 and DN p97; Dr. Hidde Ploegh (Massachusetts Institute of Technology, Cambridge, MA) for providing the HC10 mAb; Dr. H. Salomón, A. Rubio, and F. Moretti for sequencing MICA; M. Barboza, P. Do Campo, P. Maffia, and V. Pasquinelli for expert technical assistance, and M. López for performing the electronic microscopies.

Disclosures

The authors have no financial conflict of interest.

References

1. Bryceson, Y. T., M. E. March, H. G. Ljunggren, and E. O. Long. 2006. Synergy among receptors on resting NK cells for the activation of natural cytotoxicity and cytokine secretion. *Blood* 107: 159–166.
2. Cerwenka, A., and L. L. Lanier. 2001. Ligands for natural killer cell receptors: redundancy or specificity. *Immunol. Rev.* 181: 158–169.
3. Vivier, E., E. Tomasello, and P. Paul. 2002. Lymphocyte activation via NKG2D: towards a new paradigm in immune recognition? *Curr. Opin. Immunol.* 14: 306–311.
4. Raulet, D. H. 2003. Roles of the NKG2D immunoreceptor and its ligands. *Nat. Rev. Immunol.* 3: 781–790.
5. Bottino, C., R. Castriconi, L. Moretta, and A. Moretta. 2005. Cellular ligands of activating NK receptors. *Trends Immunol.* 26: 221–226.
6. Zwirner, N. W., K. Dole, and P. Stastny. 1999. Differential surface expression of MICA by endothelial cells, fibroblasts, keratinocytes, and monocytes. *Hum. Immunol.* 60: 323–330.
7. Groh, V., R. Rhinehart, H. Secrist, S. Bauer, K. H. Grabstein, and T. Spies. 1999. Broad tumor-associated expression and recognition by tumor-derived $\gamma\delta$ T cells of MICA and MICB. *Proc. Natl. Acad. Sci. USA* 96: 6879–6884.
8. Das, H., V. Groh, C. Kuijl, M. Sugita, C. T. Morita, T. Spies, and J. F. Bukowski. 2001. MICA engagement by human Vγ2Vδ2 T cells enhances their antigen-dependent effector function. *Immunity* 15: 83–93.
9. Groh, V., R. Rhinehart, J. Randolph-Habecker, M. S. Topp, S. R. Riddell, and T. Spies. 2001. Costimulation of CD8$\alpha\beta$ T cells by NKG2D via engagement by MIC induced on virus-infected cells. *Nat. Immunol.* 2: 255–260.
10. Pende, D., P. Rivera, S. Marcenaro, C. C. Chang, R. Biassoni, R. Conte, M. Kubin, D. Cosman, S. Ferrone, L. Moretta, and A. Moretta. 2002. Major histocompatibility complex class I-related chain A and UL16-binding protein expression on tumor cell lines of different histotypes: analysis of tumor susceptibility to NKG2D-dependent natural killer cell cytotoxicity. *Cancer Res.* 62: 6178–6186.
11. Gasser, S., S. Orsulic, E. J. Brown, and D. H. Raulet. 2005. The DNA damage pathway regulates innate immune system ligands of the NKG2D receptor. *Nature* 436: 1186–1190.
12. Friese, M. A., M. Platten, S. Z. Lutz, U. Naumann, S. Aulwurm, F. Bischof, H. J. Buhring, J. Dichgans, H. G. Rammensee, A. Steinle, and M. Weller. 2003. MICA/NKG2D-mediated immunogene therapy of experimental gliomas. *Cancer Res.* 63: 8996–9006.
13. Dunn, G. P., A. T. Bruce, H. Ikeda, L. J. Old, and R. D. Schreiber. 2002. Cancer immunoediting: from immunosurveillance to tumor escape. *Nat. Immunol.* 3: 991–998.
14. Khong, H. T., and N. P. Restifo. 2002. Natural selection of tumor variants in the generation of "tumor escape" phenotypes. *Nat. Immunol.* 3: 999–1005.
15. Rabinovich, G. A., E. Sotomayor, and D. Gabrilovich. 2007. Immunosuppressive strategies that are mediated by tumor cells. *Annu. Rev. Immunol.* 25: 267–296.
16. Zwirner, N. W., M. B. Fuertes, M. V. Girart, C. I. Domaica, and L. E. Rossi. 2007. Cytokine-driven regulation of NK cell functions in tumor immunity: role of the MICA-NKG2D system. *Cytokine Growth Factor Rev.* 18: 159–170.
17. Cerwenka, A., J. L. Baron, and L. L. Lanier. 2001. Ectopic expression of retinoic acid early inducible-1 gene (*RAE-1*) permits natural killer cell-mediated rejection of a MHC class I-bearing tumor in vivo. *Proc. Natl. Acad. Sci. USA* 98: 11521–11526.
18. Diefenbach, A., E. R. Jensen, A. M. Jamieson, and D. H. Raulet. 2001. Rae1 and H60 ligands of the NKG2D receptor stimulate tumour immunity. *Nature* 413: 165–171.
19. Busche, A., T. Goldmann, U. Naumann, A. Steinle, and S. Brandau. 2006. Natural killer cell-mediated rejection of experimental human lung cancer by genetic overexpression of major histocompatibility complex class I chain-related gene A. *Hum. Gene Ther.* 17: 135–146.
20. Smyth, M. J., J. Swann, E. Cretney, N. Zerafa, W. M. Yokoyama, and Y. Hayakawa. 2005. NKG2D function protects the host from tumor initiation. *J. Exp. Med.* 202: 583–588.
21. Groh, V., J. Wu, C. Yee, and T. Spies. 2002. Tumour-derived soluble MIC ligands impair expression of NKG2D and T-cell activation. *Nature* 419: 734–738.
22. Salih, H. R., H. G. Rammensee, and A. Steinle. 2002. Down-regulation of MICA on human tumors by proteolytic shedding. *J. Immunol.* 169: 4098–4102.
23. Groh, V., K. Smythe, Z. Dai, and T. Spies. 2006. Fas ligand-mediated paracrine T cell regulation by the receptor NKG2D in tumor immunity. *Nat. Immunol.* 7: 755–762.
24. Molinero, L. L., M. B. Fuertes, M. V. Girart, L. Fainboim, G. A. Rabinovich, M. A. Costas, and N. W. Zwirner. 2004. NF-κ B regulates expression of the MHC class I-related chain A gene in activated T lymphocytes. *J. Immunol.* 173: 5583–5590.
25. Kairiyama. C., I. Slavutsky, I. Larripa, V. Morvillo, A. I. Bravo, L. Bover, O. L. Podhajcer, and J. Mordoh. 1995. Biologic, immunocytochemical, and cytogenetic characterization of two new human melanoma cell lines: IIB-MEL-LES and IIB-MEL-IAN. *Pigm. Cell. Res.* 8: 121–131.
26. Guerra, L., J. Mordoh, I. Slavutsky, I. Larripa, and E. E. Medrano. 1989. Characterization of IIB-MEL-J: a new and highly heterogenous human melanoma cell line. *Pigm. Cell. Res.* 2: 504–509.
27. Paul, P., N. Rouas-Freiss, I. Khalil-Daher, P. Moreau, B. Riteau, F. A. Le Gal, M. F. Avril, J. Dausset, J. G. Guillet, and E. D. Carosella. 1998. HLA-G expression in melanoma: a way for tumor cells to escape from immunosurveillance. *Proc. Natl. Acad. Sci. USA* 95: 4510–4515.
28. Reed, J. A., E. Bales, W. Xu, N. A. Okan, D. Bandyopadhyay, and E. E. Medrano. 2001. Cytoplasmic localization of the oncogenic protein Ski in human cutaneous melanomas in vivo: functional implications for transforming growth factor β signaling. *Cancer Res.* 61: 8074–8078.
29. Zwirner, N. W., C. Y. Marcos, F. Mirbaha, Y. Zou, and P. Stastny. 2000. Identification of MICA as a new polymorphic alloantigen recognized by antibodies in sera of organ transplant recipients. *Hum. Immunol.* 61: 917–924.
30. Ackerman, A. L., A. Giodini, and P. Cresswell. 2006. A role for the endoplasmic reticulum protein retrotranslocation machinery during crosspresentation by dendritic cells. *Immunity* 25: 607–617.
31. Friese, M. A., J. Wischhusen, W. Wick, M. Weiler, G. Eisele, A. Steinle, and M. Weller. 2004. RNA interference targeting transforming growth factor-β enhances NKG2D-mediated antiglioma immune response, inhibits glioma cell migration and invasiveness, and abrogates tumorigenicity in vivo. *Cancer Res.* 64: 7596–7603.
32. Andre, D. A., J. D. Rhodes, R. L. Meisel, and J. E. Dixon. 1991. Characterization of the carboxyl-terminal sequences responsible for protein retention in the endoplasmic reticulum. *J. Biol. Chem.* 266: 14277–14282.
33. Lewis, M. J., and H. R. Pelham. 1992. Ligand-induced redistribution of a human KDEL receptor from the Golgi complex to the endoplasmic reticulum. *Cell* 68: 353–364.
34. Nilsson, T., and G. Warren. 1994. Retention and retrieval in the endoplasmic reticulum and the Golgi apparatus. *Curr. Opin. Cell Biol.* 6: 517–521.
35. Netherton, C., I. Rouiller, and T. Wileman. 2004. The subcellular distribution of multigene family 110 proteins of African swine fever virus is determined by differences in C-terminal KDEL endoplasmic reticulum retention motifs. *J. Virol.* 78: 3710–3721.
36. Haugejorden, S. M., M. Srinivasan, and M. Green. 1991. Analysis of the retention signals of two resident luminal endoplasmic reticulum proteins by in vitro mutagenesis. *J. Biol. Chem.* 266: 6015–6016.
37. Li, Z., V. Groh, R. K. Strong, and T. Spies. 2000. A single amino acid substitution causes loss of expression of a MICA allele. *Immunogenetics* 51: 246–248.
38. Zou, Y., W. Bresnahan, R. T. Taylor, and P. Stastny. 2005. Effect of human cytomegalovirus on expression of MHC class I-related chains A. *J. Immunol.* 174: 3098–3104.
39. Marsh, S. G., J. G. Bodmer, E. D. Albert, W. F. Bodmer, R. E. Bontrop, B. Dupont, H. A. Erlich, J. A. Hansen, B. Mach, W. R. Mayr, et al. 2001. Nomenclature for factors of the HLA system. *Hum. Immunol.* 62: 419–468.
40. Trombetta, E. S. 2003. The contribution of N-glycans and their processing in the endoplasmic reticulum to glycoprotein biosynthesis. *Glycobiology* 13: 77R–91R.
41. Welte, S. A., C. Sinzger, S. Z. Lutz, H. Singh-Jasuja, K. L. Sampaio, U. Eknigk, H.-G. Rammensee, and A. Steinle. 2003. Selective intracellular retention of virally induced NKG2D ligands by the human cytomegalovirus UL16 glycoprotein. *Eur. J. Immunol.* 33: 194–203.
42. Dunn, C., N. Jan Chalupny, C. L. Sutherland, S. Dosch, P. V. Sivakumar, D. C. Johnson, and D. Cosman. 2003. Human cytomegalovirus glycoprotein UL16 causes intracellular sequestration of NKG2D ligands, protecting against natural killer cell cytotoxicity. *J. Exp. Med.* 197: 1427–1439.
43. Bukau, B., J. Weissman, and A. Horwich. 2006. Molecular chaperones and protein quality control. *Cell* 125: 443–451.
44. Young, J., L. P. Kane, M. Exley, and T. Wileman. 1993. Regulation of selective protein degradation in the endoplasmic reticulum by redox potential. *J. Biol. Chem.* 268: 19810–19818.
45. Kaiser, B. K., D. Yim, I.-T. Chow, S. González, Z. Dai1, H. H. Mann, R. K. Strong, V. Groh, and T. Spies. 2007. Disulphide-isomerase-enabled shedding of tumour-associated NKG2D ligands. *Nature* 447: 482–487.
46. Raffaghello, L., I. Prigione, I. Airoldi, M. Camoriano, I. Levreri, C. Gambini, D. Pende, A. Steinle, S. Ferrone, and V. Pistoia. 2004. Downregulation and/or release of NKG2D ligands as immune evasion strategy of human neuroblastoma. *Neoplasia* 6: 558–568.
47. Le Maux Chansac, B., A. Moretta, I. Vergnon, P. Opolon, Y. Lecluse, D. Grunenwald, M. Kubin, J. C. Soria, S. Chouaib, and F. Mami-Chouaib. 2005. NK cells infiltrating a MHC class I-deficient lung adenocarcinoma display impaired cytotoxic activity toward autologous tumor cells associated with altered NK cell-triggering receptors. *J. Immunol.* 175: 5790–5798.
48. Jinushi, M., F. S. Hodi, and G. Dranoff. 2006. Therapy-induced antibodies to MHC class I chain-related protein A antagonize immune suppression and stimulate antitumor cytotoxicity. *Proc. Natl. Acad. Sci. USA* 103: 9190–9195.